



A multiobjective approach for optimal placement and sizing of distributed generators and capacitors in distribution network



Partha P. Biswas^{a,*}, R. Mallipeddi^b, P.N. Suganthan^{a,*}, Gehan A.J. Amaratunga^c

^a School of Electrical and Electronic Engineering, Nanyang Technological University, Singapore

^b Kyungpook National University, Daegu, Republic of Korea

^c Department of Engineering, University of Cambridge, UK

ARTICLE INFO

Article history:

Received 5 February 2017

Received in revised form 11 June 2017

Accepted 3 July 2017

Available online 6 July 2017

Keywords:

Radial distribution network

Distributed generator (DG)

Shunt capacitor (SC)

Power loss

Multiobjective optimization

MOEA/D algorithm

ABSTRACT

Both active and reactive power play important roles in power system transmission and distribution networks. While active power does the useful work, reactive power supports the voltage that necessitates control from system reliability aspect as deviation of voltage from nominal range may lead to inadvertent operation and premature failure of system components. Reactive power flow must also be controlled in the system to maximize the amount of real power that can be transferred across the power transmitting media. This paper proposes an approach to simultaneously minimize the real power loss and the net reactive power flow in the system when reinforced with distributed generators (DGs) and shunt capacitors (SCs). With the suggested method, the system performance, reliability and loading capacity can be increased by reduction of losses. A multiobjective evolutionary algorithm based on decomposition (MOEA/D) is adopted to select optimal sizes and locations of DGs and SCs in large scale distribution networks with objectives being minimizing system real and reactive power losses. MOEA/D is the process of decomposition of a multiobjective optimization problem into a number of scalar optimization subproblems and optimizing those concurrently. Case studies with standard IEEE 33-bus, 69-bus, 119-bus distribution networks and a practical 83-bus distribution network are performed. Output results of MOEA/D method are compared with similar past studies and notable improvement is observed.

© 2017 Elsevier B.V. All rights reserved.

1. Introduction

Competitiveness in the electric market, mitigating ever increasing load demand are some of the major challenges faced by utility companies in modern era. Augmenting capacity of transmission system may not always be a feasible or an economical solution to transmit energy to the load point. Distributed generators (DGs) installed locally near to the consumer and added capacitor bank in the system can boost the capacity, reduce losses, reduce operational cost, improve voltage profile and power quality of the network. Distributed generation can be a diesel generator, a micro-turbine run on natural gas, solar photovoltaics (PV), a wind turbine, fuel cells etc. Renewable sources like solar and wind power have added advantage of zero environmental emission. Moreover, the evolu-

tion of modular DGs calls for smaller space, less construction time and lower investment [1]. Though DG offers several benefits, it poses certain challenges when integrated in the distribution network. DG introduces bidirectional power flow in the distribution network which may possibly be designed for unidirectional power flow. This requires review and probable revamp of system protection relay co-ordination [2]. If DGs are not properly sized and located, they may lead to overvoltages and excessive power losses [3].

On the other hand, system loads specifically induction motors, transformers, transmission lines and cables are inductive in nature. These loads consume VAR and introduces lagging power factor in the system resulting in losses and poor performance of the system. Some of the DG technologies such as PV and fuel cell deliver active power only, while some are capable of supplying both active and reactive power e.g. synchronous generators driven by kinetic energy originated from various sources. Shunt capacitors are passive devices that can deliver reactive power to compensate for the lagging VAR of the network. While DGs are more effective in reducing real power loss of the system, shunt capacitors complement the

* Corresponding authors.

E-mail addresses: parthapr001@e.ntu.edu.sg (P.P. Biswas), mallipeddi.ram@gmail.com (R. Mallipeddi), epnsugan@ntu.edu.sg (P.N. Suganthan), gaja1@hermes.cam.ac.uk (G.A.J. Amaratunga).

performance of DG when used in conjunction. Researchers have demonstrated the usefulness of shunt capacitors in reducing energy loss, enhancing feeder loading capacity and improving supply reliability [4–6] of the network.

Optimal sizing and siting of both DG and shunt capacitors are of significance in improving system performance. Several literatures focused on optimal sizing and placement of DGs only in pursuit of minimizing real power loss. Analytical methods [7] and evolutionary algorithms like generic algorithm (GA) [8], particle swarm optimization (PSO) [9,10], hybrid PSO [11], hybrid ant colony optimization (ACO) and artificial bee colony (ABC) [12] have all been tried for single or multiple types of DGs. While impact of size and location of either DG or shunt capacitor has extensively been studied, a network comprising both of these items requires further attention. Naik et al. [13] took analytical approach to optimally size and locate both capacitor and DG. Aman et al. [14] adopted PSO with much improved results. In most recent papers, heuristic methods such as hybrid harmony search algorithm (HSA) and particle artificial bee colony (PABC) [15], intersect mutation differential evolution (IMDE) [16] and back-tracking search algorithm (BSA) [17] have all been applied for optimal design of capacity and placement of both DG and shunt capacitor (SC). The single objective of real power loss minimization is common in all these literatures with certain limitations on ratings of the components that are to be decided during optimization process. To reduce search space of the algorithm and hence the computational burden, Naik et al. [13] and Muthukumar et al. [15] approached location optimization based on real power loss sensitivity factors of buses. In a radial network, this factor is the ratio of change in real power loss in the line connecting the bus to change in active or reactive power of the same bus. The bus with highest real power loss sensitivity factor with respect to injection of real power into that bus and the bus with highest real power loss sensitivity factor with respect to injection of reactive power into that bus are selected as the candidate buses for accommodating DG and SC respectively.

In this present paper, multiobjective evolutionary algorithm based on decomposition (MOEA/D) is proposed with objectives of minimizing both real (active) power loss and reactive power loss in the network. Reactive power loss signifies the loss in instantaneous reactive power attributed to absorption of VAR by the inductive lines. During optimization, sensitivity factor approach is not taken and thus whole search space is explored by the algorithm to find most optimum location and rating. Besides, single objective of only minimizing the real power loss might not allocate both DG and SC at most favorable locations because the objective may fail to pinpoint places in the network where reactive power is dominant. This very fact of unidentified line sections with large amount of reactive power flow does not help to select optimum rating and best position specifically for the SC. Recalling the fact that reactive power flow incurs real power loss, by not addressing minimization of reactive power flow with imperfect placement and improper sizing of the SC, rating of the DG and its location in the network are indirectly affected. Thus, focus on reducing net reactive power flow is equally

important and if multiobjective is formulated addressing both the power components, system performance may further be enhanced. This is what has been demonstrated in this paper by applying multi-objective optimization algorithm MOEA/D to standard IEEE-33 bus, IEEE-69 bus and IEEE-119 bus systems and comparing the output results with equivalent past studies. The study is extended to a real 83-bus distribution network of Taiwan Power Company (TPC) in latter part of this literature. As an optimization algorithm, MOEA/D has some advantages over other comparable algorithms as proven and justified in [25]. The computation complexity of MOEA/D is less than multiobjective genetic local search (MOGLS) and nondominated sorting genetic algorithm II (NSGA-II). Disparate objectives can easily be accounted for in MOEA/D by simple normalization of the objectives as discussed in Section 4. MOEA/D using a small population is able to produce evenly distributed optimal solutions for multiple objectives. Due to aforementioned reasons, MOEA/D is selected as the multi-objective optimization algorithm in our study.

The organization of rest of the paper is done in following way. Section 2 includes a review of mathematical model including applicable constraints pertaining to power flow in the distribution network. In section 3, case studies performed for all the bus test systems are explained with useful numerical values. Description and application of MOEA/D algorithm are elaborated in Section 4. Section 5 discusses the simulation results followed by concluding remarks in Section 6.

2. Mathematical model

2.1. Power flow formulation

The aim of this paper is to decide proper size and discrete location of DG and SC in the network that will offer minimum power loss. Single line diagram of a simple feeder-line configuration is shown in Fig. 1. A set of recursive equations for computation of power flow is given by [18]:

$$P_{i+1} = P_i - P_{Li+1} - R_{i,i+1} \cdot \frac{P_i^2 + Q_i^2}{|V_i|^2} \tag{1}$$

$$Q_{i+1} = Q_i - Q_{Li+1} - X_{i,i+1} \cdot \frac{P_i^2 + Q_i^2}{|V_i|^2} \tag{2}$$

$$|V_{i+1}|^2 = |V_i|^2 - 2(R_{i,i+1} \cdot P_i + X_{i,i+1} \cdot Q_i) + (R_{i,i+1}^2 + X_{i,i+1}^2) \cdot \frac{P_i^2 + Q_i^2}{|V_i|^2} \tag{3}$$

where, P_i and Q_i are the real and reactive power flowing out of bus i ; P_{Li+1} and Q_{Li+1} are the real and reactive load powers at bus $i + 1$. Line section between buses i and $i + 1$ has resistance $R_{i,i+1}$ and reactance $X_{i,i+1}$. Voltage magnitude of bus i is $|V_i|$. For convergence of power flow, the power balance equations (1) and (2) must be satisfied. In addition, magnitudes of sending and receiving end bus voltages

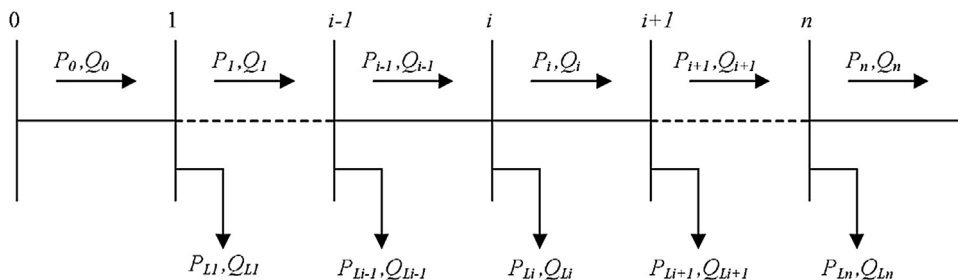


Fig. 1. Single line diagram of a radial feeder.

must satisfy equation (3). Newton-Raphson iterative method for calculation of power flow is adopted with the aid of software tool MATPOWER [32]. The power loss in the section of line connecting buses i and $i + 1$ is computed using following two equations:

$$P_{Loss}(i, i + 1) = R_{i,i+1} \cdot \frac{P_i^2 + Q_i^2}{|V_i|^2} \quad (4)$$

$$Q_{Loss}(i, i + 1) = X_{i,i+1} \cdot \frac{P_i^2 + Q_i^2}{|V_i|^2} \quad (5)$$

where, P_{Loss} is the real power loss and Q_{Loss} is the reactive power loss. Total power loss in the network is obtained by summing up all the line losses as follows:

$$TP_{Loss} = \sum_{i=0}^{n-1} P_{Loss}(i, i + 1) \quad (6)$$

$$TQ_{Loss} = \sum_{i=0}^{n-1} Q_{Loss}(i, i + 1) \quad (7)$$

where, TP_{Loss} is the total real power loss and TQ_{Loss} is the loss incurred due to reactive power throughout the network. In this study we consider DG units supplying real power with unity power factor e.g. photo-voltaic systems, micro turbines etc. Therefore, if a DG, delivering power output of P_{DG} , is added to a bus (say i -th bus), the load in that bus changes from P_{Li} to $(P_{Li} - P_{DG})$. Similarly, if m -th bus in the system has inductive load of Q_m , an addition of Q_C unit of capacitor bank alters the reactive load to $(Q_m - Q_C)$. During the search process of the algorithm it checks all possible locations with all probable ratings of the equipment to come up with best combination that results in minimum loss in the system.

2.2. Constraints

Magnitude of any bus voltage must lie within specified limits of maximum and minimum voltages. Current in any branch shall not exceed the rated capacity of the branch. Mathematically, these can be written as:

$$V_{min} \leq |V_i| \leq V_{max} \quad (8)$$

$$|I_{i,i+1}| \leq I_{i,i+1(max)} \quad (9)$$

where, V_{min} and V_{max} are the minimum and maximum allowable voltages for any bus in the network. The numerical values of these parameters for the systems are considered as 0.90 p.u. and 1.05 p.u. respectively. $|I_{i,i+1}|$ is the magnitude of current flowing in the line connecting bus i and bus $i + 1$, while $I_{i,i+1(max)}$ is the maximum permissible current through the same branch considering mainly the thermal capability limit of the line. It is mentioning worthwhile that for IEEE standard test bus systems, branch current limit is not explicitly stated. Authors in [19] made assumptions of 200A and 400A for 12.66 kV IEEE-33 bus radial distribution network, while literature [20] considered 400A, 250A and 150A. For IEEE-69 bus system also difference in presumed line capacities is observed in [16] and [20]. As current carrying capacity of a branch transpires to be a user defined parameter which might be dependent upon several other factors (e.g. whether overhead transmission line or underground cable), it does not warrant mandatory checks for its limit violation. Moreover, at medium voltage level the network current is relatively low and further augmentation with local DG relieves the burden from a line. Thereby, if base configuration of a network can support the connected load, addition of local DG or SC or both without change in load will all likely not violate line current limit. As a consequence, our algorithm presented in this paper does not check condition of line current capacity constraint.

Other constraints enforced on the algorithm are in selected ratings of DG and capacitor bank. For majority of the case studies, the maximum cumulative capacities of DGs (with unity power factor) and capacitor banks in the installation are not to exceed the limits given by [13,16]:

$$\sum_{i=1}^{N_{DG}} P_{DG,i} \leq 0.5 * \sum_{i=1}^n P_{Li} \quad (10)$$

$$\sum_{i=1}^{N_C} Q_{C,i} \leq \sum_{i=1}^n Q_{Li} \quad (11)$$

where, N_{DG} and N_C are the number of DGs and the number of SCs considered for the installation. $P_{DG,i}$ is the real power of added DG to the i -th bus, $Q_{C,i}$ is the shunt capacitor supplemented to the i -th bus. The defined constraints in equations (10) and (11) are not hard limiting. For a meaningful and rational comparison with past studies the limits are altered on case by case basis. Detail of numerical values of all these limits and relevant parameters are provided in Section 3 – ‘case studies’.

3. Case studies

The optimization study is performed on 3-standard test systems of IEEE-33 bus, IEEE-69 bus and IEEE-119 bus, and also a practical 83-bus distribution network of TPC. As a pretest of effectiveness of objectives and the algorithm, more case studies are performed for 33-bus system alongwith comparison of the results with similar past studies. Minimum values of DG and SC are set as 200 kW and 200 kVAr respectively for practicability of implementation. DG is operating at unity power factor and network is operating on full load (100%). Both DG and SC can assume any value within the specified respective range bound by minimum and maximum values. Following subsections categorize the case studies based on the above-mentioned radial bus systems.

3.1. System 1: IEEE-33 bus radial distribution network

Fig. 2 represents the standard 12.66 kV 33-bus system having 32 branches. The total load of the network is 3.72 MW and 2.3 MVAR. Line and load data are provided in [23]. Base power and base voltage of the system are 10 MVA and 12.66 kV respectively [21]. Maximum added capacity of DG is restricted to limits varied for different case studies listed in Table 1. Cumulative capacity of shunt capacitors (SCs) that can supplement the system is capped at 2.3 MVAR. Table 1 provides detail of case studies with useful numerical data. The main purpose of this paper is to find optimal size and location of both DG and SC. However, some case studies for 33-bus network (case 11–14) include either DG or SC for valid and at par comparison with past studies.

3.2. System 2: IEEE-69 bus radial distribution network

Fig. 3 indicates the standard 12.66 kV 69-bus system having 68 branches. The total load of the network is 3.8 MW and 2.69 MVAR. Line and load data are given in [23]. Base power and base voltage of the system are 10 MVA and 12.66 kV respectively [21]. Maximum added capacity of DG is restricted to limits varied slightly for several cases as in Table 2. Cumulative capacity of shunt capacitors (SCs) that can compensate the system is capped at 2.69 MVAR. Table 2 provides detail of case studies with useful numerical data.

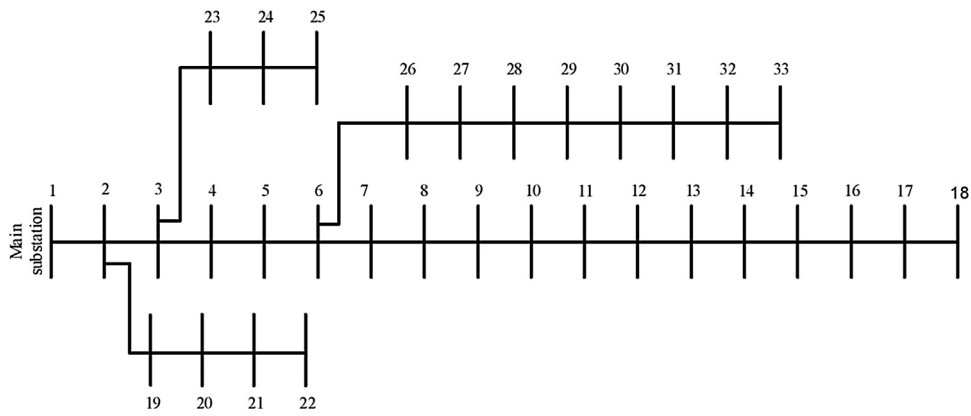


Fig. 2. Standard IEEE-33 bus test system.

Table 1
Case studies for system 1: 33-bus network.

Case no.	No. of DGs	Range of rating for each DG	Max limit of cumulative DG rating	No. of SCs	Range of rating for each SC	Max limit of cumulative SC rating
Case 11a: 1 DG only	1	0.2 – 2.0 MW	2.0 MW	–	–	–
Case 11b: 1 DG only	1	0.2 – 2.6 MW	2.6 MW	–	–	–
Case 12: 2 DGs only	2	0.2 – 2.0 MW	2.0 MW	–	–	–
Case 13: 1 SC only	–	–	–	1	0.2 – 2.3 MVar	2.3 MVar
Case 14: 2 SCs only	–	–	–	2	0.2 – 2.3 MVar	2.3 MVar
Case 15: 1 DG + 1 SC	1	0.2 – 2.5 MW	2.5 MW	1	0.2 – 2.3 MVar	2.3 MVar
Case 16: 2 DGs + 2 SCs	2	0.2 – 2.0 MW	2.0 MW	2	0.2 – 2.3 MVar	2.3 MVar

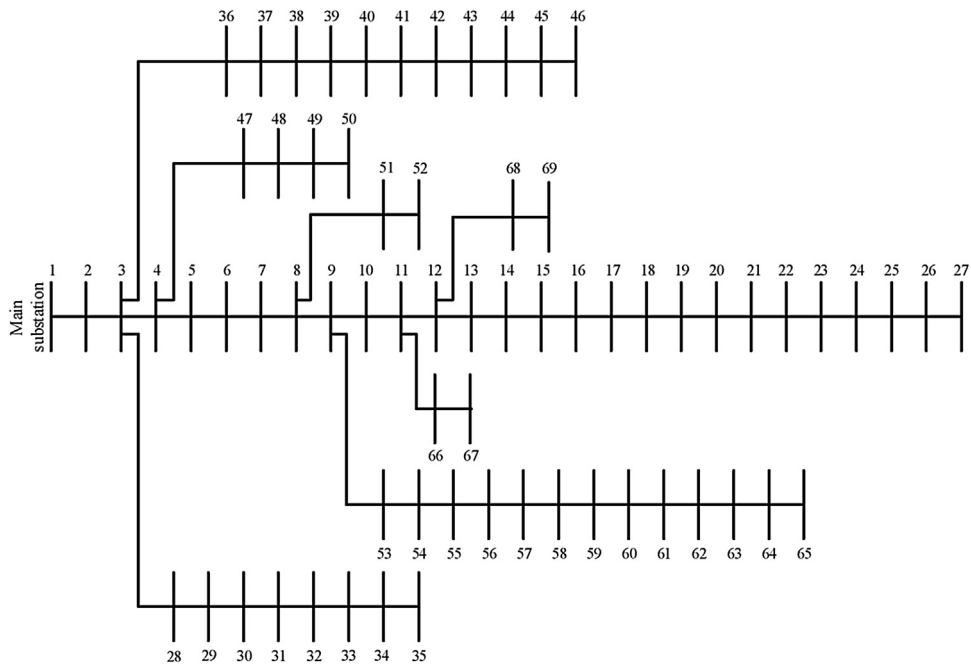


Fig. 3. Standard IEEE-69 bus test system.

Table 2
Case studies for system 2: 69-bus network.

Case no.	No. of DGs	Range of rating for each DG	Max limit of cumulative DG rating	No. of SCs	Range of rating for each SC	Max limit of cumulative SC rating
Case 21: 1 DG + 1 SC	1	0.2 – 2.25 MW	2.25 MW	1	0.2 – 2.69 MVar	2.69 MVar
Case 22: 2 DGs + 2 SCs	2	0.2 – 2.25 MW	2.25 MW	2	0.2 – 2.69 MVar	2.69 MVar
Case 23: 3 DGs + 3 SCs	3	0.2 – 3.00 MW	3.00 MW	3	0.2 – 2.69 MVar	2.69 MVar

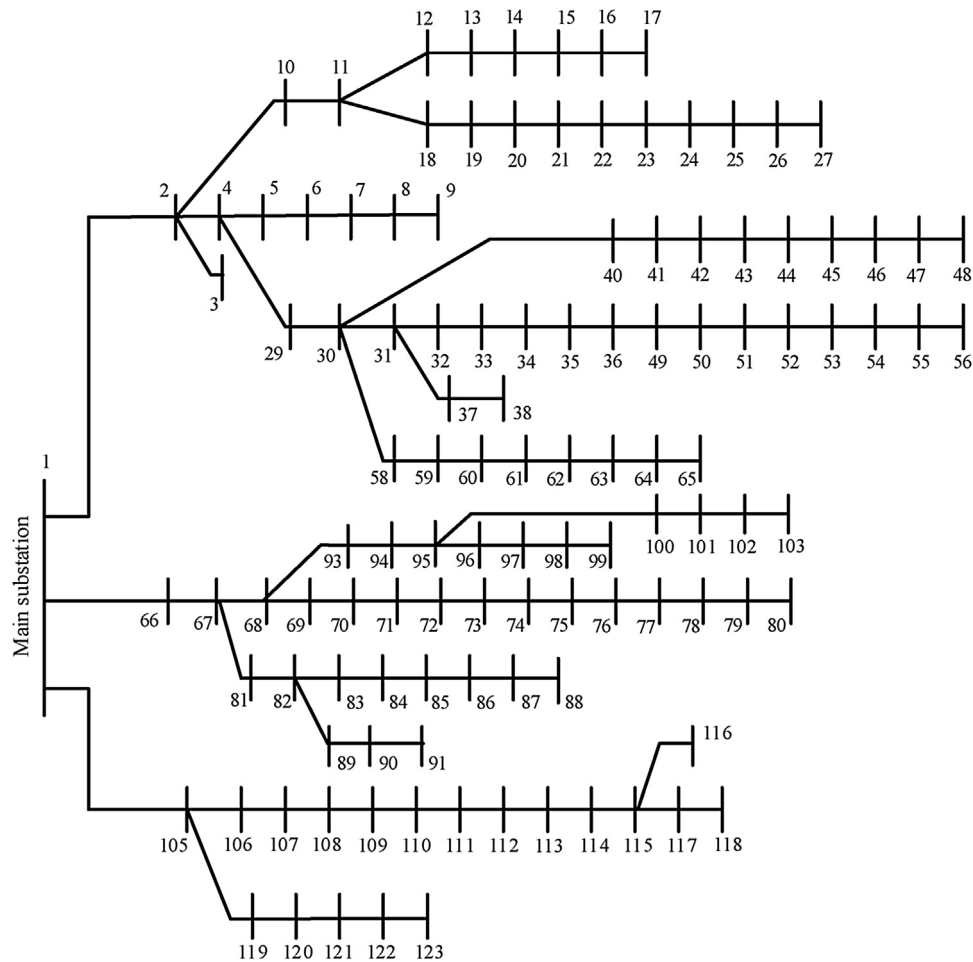


Fig. 4. Standard IEEE-119 bus test system.

Table 3
Case studies for system 3: 119-bus network.

Case no.	No. of DGs	Range of rating for each DG	Max limit of cumulative DG rating	No. of SCs	Range of rating for each SC	Max limit of cumulative SC rating
Case 31: 1 DG + 6 SCs	1	0.2 – 4.0 MW	4.0 MW	6	0.2 – 2.5 MVar	15.0 MVar
Case 32: 4 DGs + 4 SCs	4	0.2 – 2.5 MW	10.0 MW	4	0.2 – 2.5 MVar	10.0 MVar

3.3. System 3: IEEE-119 bus radial distribution network

Standard 11 kV 119-bus radial distribution system with 118 branches is shown in Fig. 4. The total load of the network is 22.71 MW and 17.04 MVar. Line and load data are same as given in [22]. Base power and base voltage of the system are 100 MVA and 11 kV respectively [15]. A limited number of studies have been carried out on 119-bus system. Therefore, maximum allowable capacities for DG and SC for various cases are judiciously chosen and listed in Table 3.

3.4. System 4: 83-bus practical distribution network

System 4 considered for study purpose is of a practical 11.4 kV distribution network of Taiwan Power Company (TPC). As depicted in Fig. 5, the network consists of 11 feeders, 83 normally closed switches and 13 normally open switches. Line and load data are provided in [18]. The total load of the network is 28.35 MW and 20.70 MVar. Literatures [18,30,31] studied reconfiguration possibilities of the network to reduce system losses. We perform case studies where DGs and SCs are optimally sized and placed in the net-

work with tie-switches of its base configuration (tie switch 84–96) remaining open. As full load of the network is higher than standard IEEE-119 bus distribution network, we formulate appropriate cases listed in Table 4. Cumulative ratings of added compensating components are kept same in both case-41 and case-42, however, in latter case the number of components is higher.

4. Application of multiobjective EA based on decomposition (MOEA/D)

4.1. Introduction and formulation of decision vector

Multi objective evolutionary algorithm (MOEA/D) decomposes a multi objective optimization problem (MOP) into a number of scalar optimization subproblems and optimizes them simultaneously [25]. The multi objective optimization (MOP), to be specific, two-objective optimization for the problem of network reinforcement with DG and SC is defined as:

$$\text{Minimize } F(x) = \{f_1(x), f_2(x)\} \quad \text{where, } f_1(x) = TP_{Loss} \quad \text{and} \quad f_2(x) = TQ_{Loss}$$

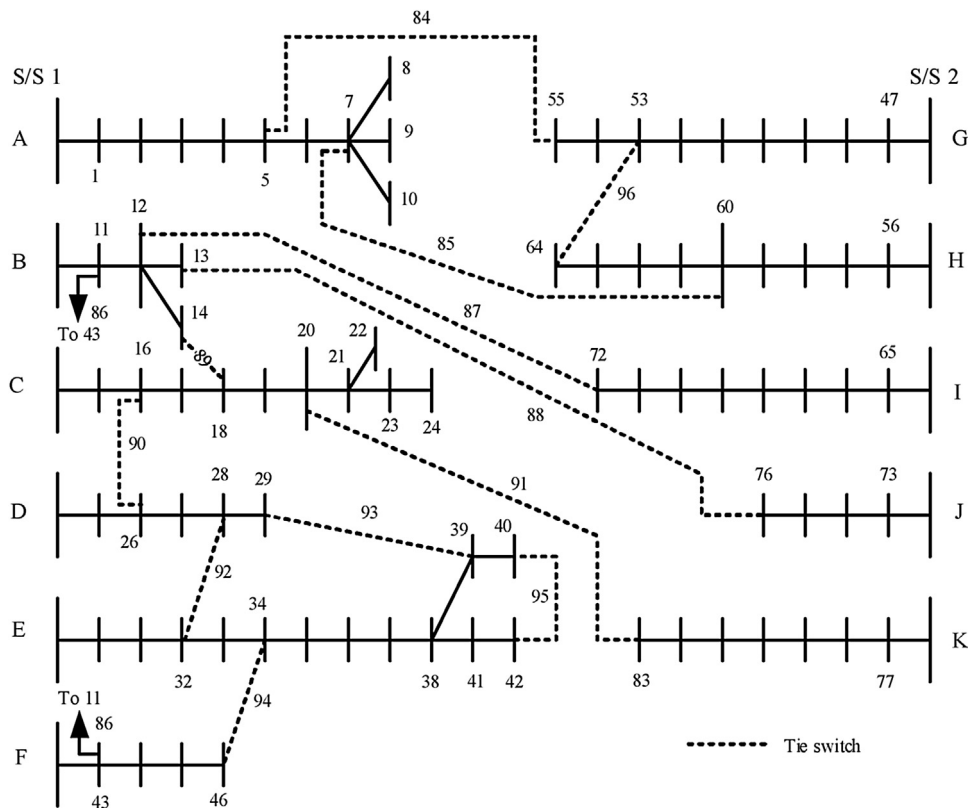


Fig. 5. 83-bus distribution network of TPC [18].

Table 4
Case studies for system 4: 83-bus TPC-network.

Case no.	No. of DGs	Range of rating for each DG	Max limit of cumulative DG rating	No. of SCs	Range of rating for each SC	Max limit of cumulative SC rating
Case 41: 4 DGs + 4 SCs	4	0.2 – 3.0 MW	12.0 MW	4	0.2 – 3.0 MVar	12.0 MVar
Case 42: 6 DGs + 6 SCs	6	0.2 – 2.0 MW	12.0 MW	6	0.2 – 2.0 MVar	12.0 MVar

where, TP_{Loss} and TQ_{Loss} are given by equations (6) and (7) respectively.

Variable $x \in \Omega$, Ω is the decision vector (variable) space. If N is the population size for the optimization problem, there will be N decision vectors x^1, x^2, \dots, x^N .

The network problem has location and size of DG and SC as the decision variables. Each decision vector x^m for $m = 1, 2, \dots, N$ is formulated as a $[2 * \text{No. of DGs} + 2 * \text{No. of SCs}]$ dimensional vector. If we consider case-16 of 33-bus system where 2 DGs and 2 SCs are to be allotted, dimension of each decision vector x^m will be $[2 * 2 + 2 * 2]$ i.e. 8. Four elements (variables) of this vector correspond to locations ranging from bus no. 1 to bus no. 33. Remaining four elements represent ratings of the DGs and SCs with probable values these may assume are bound by the range. For case-16, minimum and maximum possible values of DG are 0.2 MW and 2 MW respectively with the sum of two DGs not exceeding 2MW. Similar to DG, variables representing SCs can be assigned any value between 0.2 MVar and 2.3 MVar with sum of two SCs not exceeding 2.3 MVar. The aim is to find optimum ratings of the DGs and SCs and also their locations in the network so that the objective functions are minimized. It may be noted that during evolution through mutation and crossover value of the element of x representing location in the network may become a fraction in which case it is rounded off to the nearest integer value.

4.2. Pareto optimality

Let R^2 be the objective space for 2 objectives. Ω being the decision vector (variable) space, for $x \in \Omega, F(x) \in R^2$. We consider two objective vectors, $u, v \in R^2$. u is said to dominate v if and only if $u_i \leq v_i$ for every $i \in \{1, 2\}$ and $u_j < v_j$ for at least one index $j \in \{1, 2\}$. A point $x^* \in \Omega$ is a Pareto optimal if there is no point $x \in \Omega$ such that $F(x)$ dominates $F(x^*)$ [26]. $F(x^*)$ is called Pareto optimal (objective) vector. In other words, any improvement in a Pareto optimal point in one objective must lead to deterioration of other objective(s). The set of all the Pareto optimal points is called Pareto set (PS) and the set of all the Pareto optimal objective vectors is the Pareto front (PF) [28].

MOEA/D is extensively applied to problems with conflicting objectives, which imply betterment of one objective leads to deterioration of others. Out of the Pareto set obtained by the algorithm, designer picks an optimal solution, often the one that compromises all the objectives to a certain extent in the problem. Like many other algorithms, MOEA/D has its limitations. The possibility of non-uniform distribution in Pareto front and weak convergence of the algorithm are some of the few drawbacks. While improved variant of MOEA/D is proposed in [29], the shortcomings of past algorithm hardly affect the results in our research study presented in this paper. The two objectives considered for the network problem here are not completely contradicting as addition of either DG or SC

Table 5
MOEA/D optimization data.

Parameter	Value
Population size, N	600
Number of weight vectors, N	600
Neighborhood size, T	0.1 N
Probability to update the neighbor (or the whole population otherwise), δ	0.9
Max number of positions replaced by better new solution in each subproblem at every generation, n_r	0.01* N
Maximum number of function evaluation, $Maxeval$	100000
Crossover rate, CR	0.5
Mutation factor, F	0.5
Distribution index [26]	20

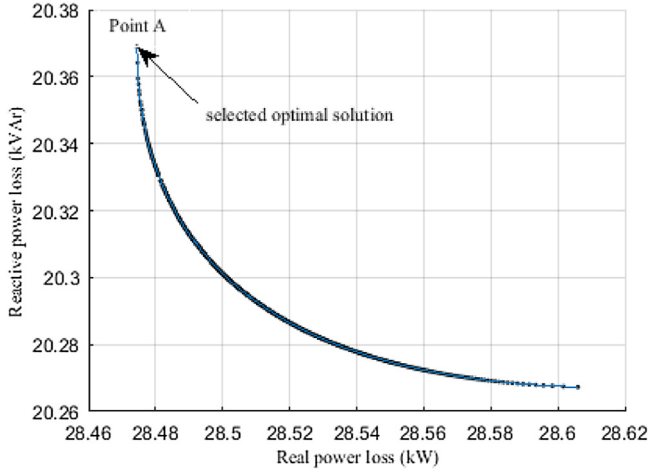


Fig. 6. Plot of Pareto front for case-16 of 33-bus test system.

reduces loss in the system, however to a varying degree. Therefore, Pareto front converges to a very narrow zone and a smaller population size (N) than what has been considered (in Table 5) shall be able to attain the desired optimal results. Fig. 6 represents the Pareto front of optimal solutions for case-16 (2 DGs + 2 SCs) in 33-bus network. The solutions for optimal real power loss lie in the range of [28.47, 28.61] kW and the solutions for optimal reactive power loss are in the range of [20.27, 20.37] kVAr. As main objective of the problem is to achieve lowest possible real power loss for the network, from narrow range of selection, the chosen Pareto optimal (objective) solution is 'point A' (28.47 kW, 20.37 kVAr) in the graph. The decision vector leading to solution 'point A' constitutes of elements signifying the optimal location and rating of DG and SC. If x^{opt} is the decision vector corresponding to the optimal solution found by the algorithm, for case-16 it would be an 8-dimensional vector with four elements representing optimal DG location and rating as [bus 13, 840 kW, bus 30, 1140 kW] and balance four denoting optimum SC location and rating as [bus 12, 453 kVAr, bus 30, 1040 kVAr]. Similar approach is taken for selection of optimal solutions of all other cases considered under the purview of this literature and results are included in section 5.

4.3. Decomposition approach

MOEA/D decomposes the approximation of PF into a number of scalar optimization subproblems [27]. Out of many variants of MOEA/D, the one with dynamic resource allocation (MOEA/D-DRA) [26] is applied here. To decompose the MOP, we require N evenly spread weight vectors $\lambda^1, \lambda^2, \dots, \lambda^N$. In this specific problem of network, $N=600$ is considered with each of the vector being 2 dimensional for the two objectives i.e. $\lambda^m = (\lambda_1^m, \lambda_2^m)^T$ for $m=1, 2, \dots, N$ and $\lambda_1^m + \lambda_2^m = 1$.

Let $z^* = (z_1^*, z_2^*)^T$ be the minimum objective value vector which will be treated as reference point and the elements of this vector are calculated as $z_1^* = \min \{f_1(x) | x \in \Omega\}$ and $z_2^* = \min \{f_2(x) | x \in \Omega\}$. After decomposition into N subproblems, the objective function of m -th subproblem is:

$$\min g^{te}(x | \lambda^m, z^*) = \max \left\{ \begin{array}{l} \lambda_1^m | f_1(x) - z_1^* \\ \lambda_2^m | f_2(x) - z_2^* \end{array} \right\} \quad (12)$$

z^* is often unknown beforehand and during the search process the algorithm uses the lowest values of $f_1(x)$ and $f_2(x)$ found so far to substitute z_1^* and z_2^* respectively in the decomposed objective subproblems. MOEA/D minimizes all the N objective functions simultaneously in a single run. Each subproblem is optimized by using information mainly from its neighboring subproblems. In MOEA/D-DRA, different subproblems are given varying computational effort based on utility of the sub-problem [26].

Normalization of the objectives is also an important aspect of MOEA/D. The objectives in the network problem are disparate as numerical values of real power loss TP_{Loss} and loss due to reactive power flow TQ_{Loss} can be quite different. The intention of normalization is to bring the values of both objectives within range 0–1. To implement this, the decomposed objective function in Eq. (12) for continuous MOP is to be modified as:

$$\min g^{te}(x | \lambda^m, z^*, z^{nad}) = \max \left\{ \begin{array}{l} \lambda_1^m \left| \frac{f_1(x) - z_1^*}{z_1^{nad} - z_1^*} \right| \\ \lambda_2^m \left| \frac{f_2(x) - z_2^*}{z_2^{nad} - z_2^*} \right| \end{array} \right\} \quad (13)$$

where, $z^{nad} = (z_1^{nad}, z_2^{nad})^T$ is the vector of maximum values of $f_1(x)$ and $f_2(x)$ and similar to z^* , z^{nad} is also evaluated by the algorithm during the search process using maximum values of $f_1(x)$ and $f_2(x)$.

During the search process MOEA/D-DRA with Tchebycheff approach [28] maintains:

- A population of N vectors x^1, x^2, \dots, x^N
- Function values of FV^1, FV^2, \dots, FV^N where, $FV^m = \{f_1(x^m), f_2(x^m)\}$ for $m=1, 2, \dots, N$.
- $z^* = (z_1^*, z_2^*)^T$, where z_1^* and z_2^* are the minimum values found thus far evaluating $f_1(x)$ and $f_2(x)$.
- $z^{nad} = (z_1^{nad}, z_2^{nad})^T$, where z_1^{nad} and z_2^{nad} are the maximum values found till now evaluating functions $f_1(x)$ and $f_2(x)$.
- Utility of the subproblems, π^m for $m=1, 2, \dots, N$.
- Current generation number gen .

4.4. MOEA/D-DRA algorithm

Input: (i) MOP (ii) a stopping criteria, $Maxeval$ (iii) Number of subproblems, N (iv) A uniform spread of N weight vectors, $\lambda^1, \lambda^2, \dots, \lambda^N$ (v) T : the number of the weight vectors in the neighborhood of each weight vector.

Output: $\{x^1, x^2, \dots, x^N\}$ and $\{f_1(x^m), f_2(x^m)\}$ for $m=1, 2, \dots, N$.

Step 1 – Initialization: Initialize decision vectors as described in Section 4.1. Initialize N uniformly spread weight vectors, z^*, z^{nad} . Set generation counter $gen=0$ and utility function $\pi^m=1$ for all subproblems. Define constraint if any, limits on bus voltage for the problem.

Step 2–Selection of subproblems and update of solutions: For each weight vector, its N_S neighborhood is the set of N_S closest weight vectors to it. In sync with that, each solution and each subproblem have their N_S neighborhoods. Selection of subproblems is done based on utility value using 10-tournament selection method [26], usually 20% of the total population is identified in the process

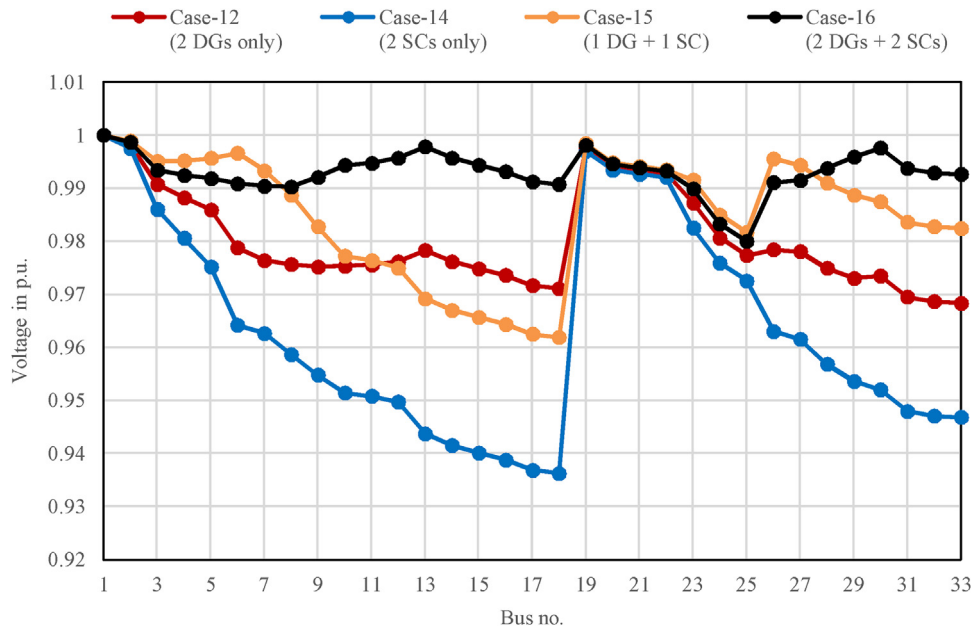


Fig. 7. Bus voltage profiles of 33-bus system for different case studies.

in each generation. A set of the current solutions corresponding to the selected indices of subproblems is picked up in that generation. For each selected solution x^m , MOEA/D-DRA does the following [27]:

1. Set the mating and update range P to be the T -neighborhood of x^m with a large probability δ , and the whole population otherwise.
2. Randomly select three current solutions from P .
3. Apply genetic operators with pre-defined crossover rate CR and mutation factor F on the above selected solutions to generate a new solution y [26]. Check range bounds for y and repair if necessary. Compute objective $F(y)$. Check for violation of any constraint.
4. Replace a small number (n_r) of solutions in P by y if y yields better than current FV of related subproblem.

No solution will be replaced in step 4 if y is not better than any solution in P for its subproblem or if any constraint is not satisfied. The update is considered to be a failure if such a case happens, else it is successful.

Step 3—Stop if stopping criteria i.e. *Maxeval* (maximum number of function evaluation) is reached

Step 4— $gen = gen + 1$. At every 50-th *gen* utility function is updated [26]. Go to **Step 2**.

The selected parameters of MOEA/D for the network problem are given in Table 5.

The proposed algorithms are developed using MATLAB software and simulations are carried out on a computer with Intel Core i5 CPU @2.7 GHz and 4GB RAM. Simulation results are discussed in subsequent section.

5. Results and comparison

The results of application of the multiobjective optimization algorithm are tabulated, as well as detail system by system explanation and comparative analysis are provided in this section. Configuration of each case study for a system is listed in the table. For detail description of case studies, Section 3 is to be referred. Selection of *Pareto optimal* solution for a case study is explained under Section 4.2.

5.1. System 1: IEEE-33 bus radial distribution network

Table 6 summarizes results and comparison with most recently applied methods for all the case studies performed for 33-bus test system. A quick look at the tabulated results reveals that MOEA/D is far superior to analytical approach adopted in [13]. The selection limits of equipment are same, however MOEA/D correctly selects higher rated equipment as prime objective is minimization of real power loss. For case-11b and case-12 when only DG is added to the network, output results of MOEA/D, IMDE, BSA and hybrid algorithms for deciding place and size of the equipment are quite similar. In case-12, loss has been recalculated for IMDE algorithm with the rating and location proposed for the DG by the algorithm in [16]. A little change is observed from reported value which might be for numerical approximation in p.u. conversion. The purpose is to highlight that MOEA/D proposed bus-13 is preferred to IMDE proposed bus-14 for allocating DGs in case-12. When 2 nos. properly sized SCs are to be allotted in case-14, a change in location is suggested by MOEA/D from what has been recommended by IMDE for comparable rating of one SC.

MOEA/D with multiobjective performs much better than PSO as results of case-15 show. The recorded system loss is higher using PSO [14] with higher ratings of equipment. Multiobjective outperforms in a notable manner in case-16 when more numbers of correctly sized DGs and SCs are to be allocated. An obvious reason is for accounting losses due to both active power and reactive power. Amin et al. [16] has given certain weightage on system loss due to reactive power flow in the objective function to arrive at practically good solutions. However, superiority of MOEA/D lies in its ability to optimize multiple objectives which may be contradicting. With almost similar ratings of the components as in [16] but with little reshuffle in positioning, the system real power loss is brought down further by about 11.25%. BSA algorithm could lower real power loss to an extent, however selected DG size is much larger. In summary, as far as the objective of this optimization is concerned, overall assessment of Table 6 for 33-bus test system discloses that for all cases, proposed size and location by MOEA/D algorithm results in real power loss less than any alternate selection and arrangement suggested by an analogous algorithm.

Table 6
Simulation results for system 1: 33-bus network.

Case description	Parameter	Various optimization methods					
		MOEA/D	IMDE [16]	Analytical [13]	PSO [14]	BSA [17]	Hybrid [15]
Case-11a (1 DG only)	Real power loss, kW	107.96	–	142.34	–	–	–
	DG size in kW (bus no.)	2000 (7)	–	1000 (18)	–	–	–
	Min bus voltage in p.u. (bus no.)	0.9454 (18)	–	0.9311 (33)	–	–	–
Case-11b (1 DG only)	Real power loss, kW	103.95	–	–	–	103.96	111.03
	DG size in kW (bus no.)	2575 (6)	–	–	–	2575.3 (6)	2598 (6)
	Min bus voltage in p.u. (bus no.)	0.9511 (18)	–	–	–	not reported	0.9425 (18)
Case-12 (2 DGs only)	Real power loss, kW	85.91	86.12 ^a	–	–	87.16	–
	DG size in kW (bus no.)	844 (13), 1156 (30)	840 (14), 1130 (30)	–	–	851.6 (13), 1157.6 (30)	–
	Min bus voltage in p.u. (bus no.)	0.9684 (33)	0.9675 ^a (33)	–	–	not reported	–
Case-13 (1 SC only)	Real power loss, kW	143.59	–	164.6	–	–	–
	SC size in kVAr (bus no.)	1252 (30)	–	1000 (33)	–	–	–
	Min bus voltage in p.u. (bus no.)	0.9261 (18)	–	0.9165 (18)	–	–	–
Case-14 (2 SCs only)	Real power loss, kW	135.74	139.7	–	–	–	–
	SC size in kVAr (bus no.)	469 (12), 1057 (30)	475 (14), 1037 (30)	–	–	–	–
	Min bus voltage in p.u. (bus no.)	0.9363 (18)	0.942 (18)	–	–	–	–
Case-15 (1 DG + 1 SC)	Real power loss, kW	51.79	–	–	59.7	58.37	58.45
	DG size in kW (bus no.)	2500 (6)	–	–	2511 (6)	2500 (6)	2531 (6)
	SC size in kVAr (bus no.)	1250 (30)	–	–	1457 (30)	1243.6 (6)	1250 (30)
	Min bus voltage in p.u. (bus no.)	0.9620 (18)	–	–	0.955 (18)	not reported	0.9536 (18)
Case-16 (2 DGs + 2 SCs)	Real power loss, kW	28.47	32.08	84.28	–	30.87	–
	DG size in kW (bus no.)	840 (13), 1140 (30)	1080 (10), 896.4 (31)	447 (18), 559 (17)	–	860 (13), 1310.5 (30)	–
	SC size in kVAr (bus no.)	453 (12), 1040 (30)	254.8 (16), 932.3 (30)	400 (33), 500 (32)	–	334.8 (14), 899.8 (30)	–
	Min bus voltage in p.u. (bus no.)	0.9800 (25)	0.979 (25)	0.961 (30)	–	not reported	–

^a Values are recalculated with same proposed ratings of DG and SC.

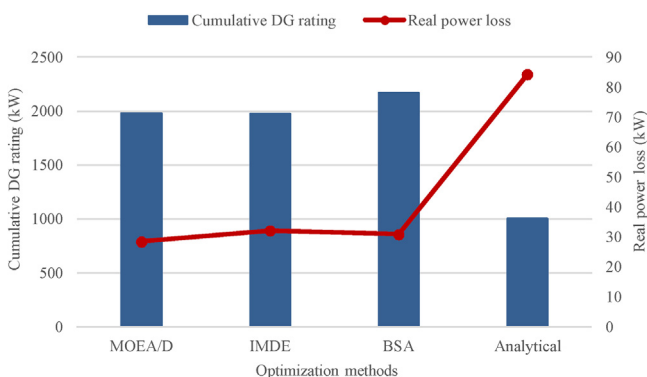


Fig. 8. Selected cumulative DG rating vs real power loss with various optimization methods for case-16 of 33-bus system.

Voltage profiles of buses for selected cases of 33-bus system are represented in Fig. 7. All bus voltages are found to be within allowable limits. Best profile is justifiably obtained with 2 DGs + 2 SCs. Furthermore, selection of 2 DGs (case-12) turns out to be a better choice than 2 SCs (case-14) in the context of voltage uniformity. This is because network real power is higher than the reactive power and hence compensation of real power has greater influence in controlling losses and voltage in the system. Though it may be noted that cost of installation of DG is much more than the cost of installation of SC. DG requires electricity generating source, associated interface, control and protective equipment commensurate with the capacity of the DG. Enhancing rating of DG implies augmenting ratings of all related accessories. Investment cost of diesel generator based 1 MW DG is found to be 50 times higher than the investment cost of 1 MVar capacitor bank [24]. Fig. 8 shows comparison of cumulative DG rating versus network real power loss achieved with various algorithms for case-16 with 2 DGs + 2 SCs of 33-bus system. Loss by MOEA/D method is the lowest with DG rating same as in IMDE. Selected rating of DG is high in case of BSA with reasonably low loss figure. Analytical method selects lowest

DG rating, but loss is almost 3-times higher than the loss given by MOEA/D algorithm. Comparison on this aspect shows the effectiveness of simultaneous minimization of real and reactive power losses. Selection of proper rating and location of SC helps to have same or lower ratings for the DGs resulting in lower real power loss in the network.

5.2. System 2: IEEE-69 bus radial distribution network

Results of case studies for 69-bus test system and comparison with other recently applied methods are provided in Table 7. In case-21 of single DG and single SC, MOEA/D selects larger rating of DG when compared with PSO method, but network real power loss is further reduced by about 10.5% with slightly improved voltage profile. Major improvement in loss value is seen for case-22 with 2 DGs+2 SCs. With almost similar ratings of the equipment but change in placement of these, brings the loss down by about extra 48%. Kanwar et al. [20] in applying improved particle swarm optimization (IPSO) considered reconfiguration of the network after optimal sizing of DG and SC. The output results included in this table for case-23 are recalculated without network reconfiguration but with the proposed ratings of the equipment by IPSO method. These results when assessed against MOEA/D are found to be almost same as far as total rating of the added components is concerned. With redistribution of total capacity of the equipment and change in placement in the network, loss is marginally reduced by MOEA/D algorithm.

Fig. 9 shows voltage profiles for various case studies performed for the 69-bus radial distribution network. The profile is rightly more uniform and even for case-22 when 2 DGs+2 SCs are added than for case-21 when 1 DG+1 SC are used. However, boosting network capacity with even more numbers of equipment may drive the network to voltage overshoot as can be observed in case-23. Therefore, careful judgement is necessary as adding large number of equipment may not be economically viable, technically feasible or may well turn out to be literally ineffective.

Table 7
Simulation results for system 2: 69-bus network.

Case description	Parameter	Various optimization methods			
		MOEA/D	IMDE [16]	PSO [14]	IPSO [20]
Case-21 (1 DG + 1 SC)	Real power loss, kW	23.17	–	25.90	–
	DG size in kW (bus no.)	1829 (61)	–	1566 (61)	–
	SC size in kVAr (bus no.)	1301 (61)	–	1401.3 (61)	–
	Min bus voltage in p.u. (bus no.)	0.9731 (27)	–	0.970 (27)	–
Case-22 (2 DGs + 2 SCs)	Real power loss, kW	7.20	13.83	–	–
	DG size in kW (bus no.)	1731 (61), 520 (17)	1738 (62), 479 (24)	–	–
	SC size in kVAr (bus no.)	353 (17), 1239 (61)	109 (63), 1192 (61)	–	–
	Min bus voltage in p.u. (bus no.)	0.9943 (69)	0.9915 (68)	–	–
Case-23 (3 DGs + 3 SCs)	Real power loss, kW	4.25	–	–	4.37 ^a
	DG size in kW (bus no.)	495 (11), 379 (18), 1675 (61)	–	–	557 (11), 321 (21), 1672 (61)
	SC size in kVAr (bus no.)	375 (11), 230 (21), 1196 (61)	–	–	300 (11), 300 (18), 1200 (61)
	Min bus voltage in p.u. (bus no.)	0.9943 (50)	–	–	0.9943 ^a (50)

^a Values are recalculated with same proposed ratings of DG and SC but without network re-configuration.

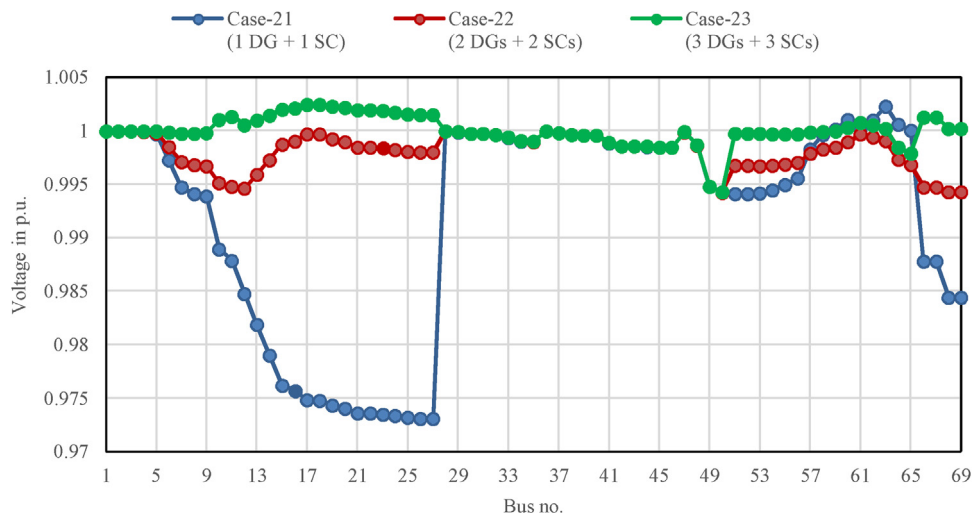


Fig. 9. Bus voltage profiles of 69-bus system for different case studies.

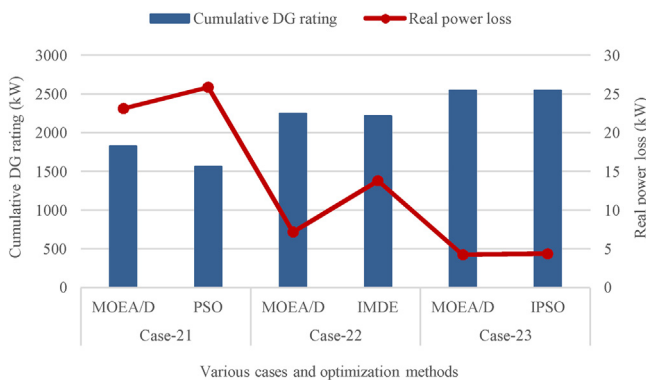


Fig. 10. Selected cumulative DG rating vs real power loss with various optimization methods for case studies of 69-bus system.

Fig. 10 represents cumulative DG rating versus real power loss for various case studies of 69-bus test system. Lowest loss is achieved by MOEA/D algorithm with almost same rating of DG with exception in case-21. Selected DG rating by MOEA/D is higher than what has been recommended by PSO method, nevertheless, MOEA/D arrives at approximately 10.5% lower loss figure.

5.3. System 3: IEEE-119 bus radial distribution network

A summary of results alongwith comparison with a similar past study is presented in Table 8. In case-31, MOEA/D selects a DG capacity of 2913 kW and cumulative capacitor rating of 10590 kVAr. Hybrid algorithm proposes 2650 kW for DG and 13200 kVAr for SCs. Loss achieved by MOEA/D algorithm is about 46 kW less than what has been achieved by Hybrid algorithm. It transpires that augmenting DG capacity by 263 kW (i.e. 2913–2650 kW) is worth than adding capacitor bank of 2610 kVAr (i.e. 13200–10590 kVAr). An additional study case-32 is proposed without violating any compensating capacity constraints. With the arrangement proposed in case-32, the loss could be drastically reduced alongside more uniform voltage profile of the network.

Fig. 11 indicates the voltage profiles for different case studies performed for IEEE-119 bus test system. Voltages of all the buses are within allowable limits. A smoother voltage profile is obtained in case-32 with more evenly rated DGs and SCs distributed throughout the network.

5.4. System 4: 83-bus TPC-network

Table 9 presents a summary of results from the case studies performed for 83-bus practical TPC distribution network. All 13 tie switches (no. 84–96) are considered open for the case studies with

Table 8
Simulation results for system 3: 119-bus network.

Case description	Parameter	Various optimization methods	
		MOEA/D	Hybrid [15]
Case-31 (1 DG + 6 SCs)	Real power loss, kW	595.74	641.61
	DG size in kW (bus no.)	2913 (74)	2650 (76)
	SC size in kVAr (bus no.)	1509 (42), 2500 (52), 1513 (77), 1645 (83), 1103 (100), 2320 (115)	4400 (29), 2900 (35), 1850 (73), 1200 (89), 500 (88), 2350 (115)
	Min bus voltage in p.u. (bus no.)	0.9325 (116)	0.9317 (118)
Case-32 (4 DGs + 4 SCs)	Real power loss, kW	271.41	–
	DG size in kW (bus no.)	2500 (52), 2500 (75), 1840 (100), 2500 (115)	–
	SC size in kVAr (bus no.)	2486 (52), 1732 (75), 1700 (83), 2348 (115)	–
	Min bus voltage in p.u. (bus no.)	0.9603 (48)	–

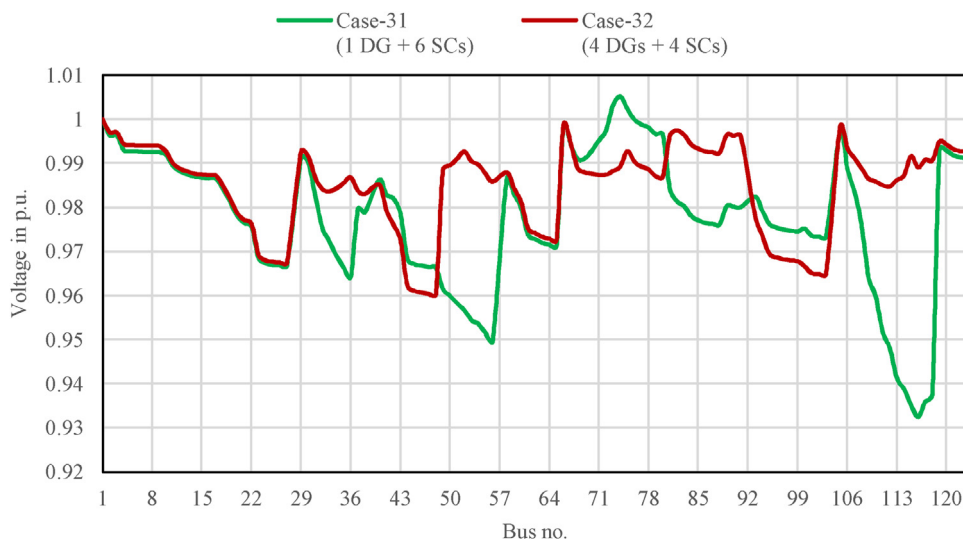


Fig. 11. Bus voltage profiles of 119-bus system for different case studies.

Table 9
Simulation results for system 4: 83-bus TPC-network.

Case description	Parameter	MOEA/D
Base case (without DG and SC)	Real power loss, kW	531.99
	Min bus voltage in p.u. (bus no.)	0.9285 (9)
Case-41 (4 DGs + 4 SCs)	Real power loss, kW	217.77
	DG size in kW (bus no.)	3000 (6), 2945 (33), 2507 (71), 3000 (79)
	SC size in kVAr (bus no.)	2260 (6), 2841 (31), 1923 (71), 2539 (79)
	Min bus voltage in p.u. (bus no.)	0.9651 (24)
Case-42 (6 DGs + 6 SCs)	Real power loss, kW	151.43
	DG size in kW (bus no.)	2000 (7), 2000 (19), 2000 (34), 2000 (53), 2000 (71), 2000 (81)
	SC size in kVAr (bus no.)	2000 (7), 2000 (19), 2000 (33), 1720 (52), 1936 (71), 2000 (79)
	Min bus voltage in p.u. (bus no.)	0.9675 (64)

100% loading onto the network. Loss in the base case, where no DG or SC is installed in the network, is 531.99 kW. In case-41 with the proposed ratings and locations of 4DGs and 4SCs, the network loss is brought down to 217.77 kW. Minimum voltage of the network is improved from 0.9285 p.u. to 0.9651 p.u. The maximum allowable individual ratings of 3 MW for the DG and 3 MVar for the SC are not fully utilized. Much lower network loss can be achieved with higher number of DGs and SCs as seen in case-42. The loss is reduced by about 71.5% than the base case with MOEA/D suggested ratings and locations of the added components. A more uniform selection of ratings is observed in case-42. In general, it is noted that higher the number of suitably rated components, larger is the reduction in

system loss if the components are distributed uniformly throughout the network. However, it is not practical to increase the number of devices beyond a certain extent. Availability of bus and components for fixing, the cost of procurement and installation dictate the number of compensating devices to be added. Detail technical and commercial evaluation is necessary on case by case basis. For the TPC-network under study, results of case-42 can be adopted for augmentation of capacity and reliability of the network. Fig. 12 shows bus voltage profiles for case-41 and case-42. As expected, the profile is more uniform in case-42 with higher number of evenly rated components installed in the network.

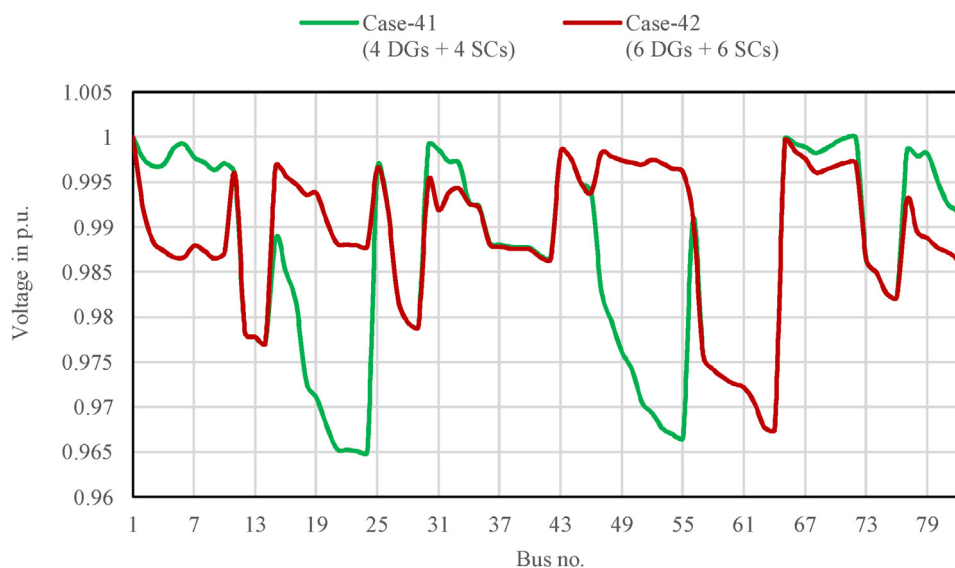


Fig. 12. Bus voltage profiles of 83-bus TPC network for different case studies.

6. Conclusion

This paper discusses in detail the application and usefulness of MOEA/D optimization algorithm for deciding the rating and the location of DG and SC simultaneously in the network to reduce real power loss. It has also been substantiated that control of reactive power flow in the network is also vital to reduce real power loss. Upgrade of distribution or transmission system may not always be a feasible option. So, proper size and judicious allocation DG and SC defer impending upgradation of the transmission or the distribution system by increasing its loading capability. On the optimization aspect, consideration of multiple objectives is highly effective especially when large numbers of compensating DGs and SCs are present in the system. MOEA/D performs arguably best among equivalent optimization methods. Reduction in loss has been established in all the cases studied under the scope of this literature. Cutting down loss by any amount is of technical and commercial advantage. Energy signifies cost to the utility and to the consumer and any saving in energy when compounded annually turns out to be a substantial amount. Moreover, reduction in real power loss means lower heat generation as a direct consequence. Thus, reliability of system components is also enhanced due to long term positive effect of lesser heat emission.

Acknowledgement

This project is funded by the National Research Foundation Singapore under its Campus for Research Excellence and Technological Enterprise (CREATE) program.

References

- [1] Prem Prakash, Dheeraj K. Khatod, Optimal sizing and siting techniques for distributed generation in distribution systems: a review, *Renew. Sustain. Energy Rev.* 57 (2016) 111–130.
- [2] A. Gopalan Sachit, Victor Sreeram, and Herbert HC Lu: a review of coordination strategies and protection schemes for microgrids, *Renew. Sustain. Energy Rev.* 32 (2014) 222–228.
- [3] Ahmad Rezaee, Jordehi, Allocation of distributed generation units in electric power systems: a review, *Renew. Sustain. Energy Rev.* 56 (2016) 893–905.
- [4] Sayyad Nojavan, Mehdi Jalali, Kazem Zare, Optimal allocation of capacitors in radial/mesh distribution systems using mixed integer nonlinear programming approach, *Electr. Power Syst. Res.* 107 (2014) 119–124.
- [5] Sultana Sneha, Provas Kumar Roy, Optimal capacitor placement in radial distribution systems using teaching learning based optimization, *Int. J. Electr. Power Energy Syst.* 54 (2014) 387–398.
- [6] A.H. Etemadi, M. Fotuhi-Firuzabad, Distribution system reliability enhancement using optimal capacitor placement, *IET Gener., Transm. Distrib.* 2.5 (2008) 621–631.
- [7] Rajkumar Viral, D.K. Khatod, An analytical approach for sizing and siting of DGs in balanced radial distribution networks for loss minimization, *Int. J. Electr. Power Energy Syst.* 67 (2015) 191–201.
- [8] T.R. Ayodele, A.S.O. Ogunjuyigbe, O.O. Akinola, Optimal location, sizing, and appropriate technology selection of distributed generators for minimizing power loss using genetic algorithm, *J. Renew. Energy* 2015 (2015).
- [9] Peyman Karimyan, et al., Long term scheduling for optimal allocation and sizing of DG unit considering load variations and DG type, *Int. J. Electr. Power Energy Syst.* 54 (2014) 277–287.
- [10] Satish Kansal, Vishal Kumar, Barjeev Tyagi, Optimal placement of different type of DG sources in distribution networks, *Int. J. Electr. Power Energy Syst.* 53 (2013) 752–760.
- [11] M.M. Aman, G.B. Jasmon, A.H.A. Bakar, H. Mokhlis, A new approach for optimum simultaneous multi-DG distributed generation Units placement and sizing based on maximization of system loadability using HPSO (hybrid particle swarm optimization) algorithm, *Energy* 66 (2014) 202–215.
- [12] M. Kefayat, A. Lashkar Ara, S.A. Nabavi Niaki, A hybrid of ant colony optimization and artificial bee colony algorithm for probabilistic optimal placement and sizing of distributed energy resources, *Energy Convers. Manage.* 92 (2015) 149–161.
- [13] S. Gopiya Naik, D.K. Khatod, M.P. Sharma, Optimal allocation of combined DG and capacitor for real power loss minimization in distribution networks, *Int. J. Electr. Power Energy Syst.* 53 (2013) 967–973.
- [14] M.M. Aman, G.B. Jasmon, K.H. Solangi, A.H.A. Bakar, H. Mokhlis, Optimum simultaneous DG and capacitor placement on the basis of minimization of power losses, *Int. J. Comp. Electr. Eng.* 5 (5) (2013) 516.
- [15] K. Muthukumar, S. Jayalalitha, Optimal placement and sizing of distributed generators and shunt capacitors for power loss minimization in radial distribution networks using hybrid heuristic search optimization technique, *Int. J. Electr. Power Energy Syst.* 78 (2016) 299–319.
- [16] Khodabakhshian Amin, Mohammad Hadi Andishgar, Simultaneous placement and sizing of DGs and shunt capacitors in distribution systems by using IMDE algorithm, *Int. J. Electr. Power Energy Syst.* 82 (2016) 599–607.
- [17] Waleed Fadel, Ulas Kilic, Sezai Taskin, Placement of Dg, Cb, and Tcsc in radial distribution system for power loss minimization using back-tracking search algorithm, *Electr. Eng.* (2016) 1–12.
- [18] Ji-Pyng Chiou, Chung-Fu Chang, Su. Ching-Tzong, Variable scaling hybrid differential evolution for solving network reconfiguration of distribution systems, *IEEE Trans. Power Syst.* 20.2 (2005) 668–674.
- [19] M.R.M. Cruz, D.Z. Fitiwi, S.F. Santos, J.P.S. Catalão, Influence of distributed storage systems and network switching/reinforcement on RES-based DG integration level, in: *European Energy Market (EEM)*, 2016 13th International Conference on the IEEE, IEEE June 2016, 2016, pp. 1–5.
- [20] N. Kanwar, N. Gupta, K.R. Niazi, A. Swarnkar, Improved meta-heuristic techniques for simultaneous capacitor and DG allocation in radial distribution networks, *Int. J. Electr. Power Energy Syst.* 73 (2015) 653–664.
- [21] Sivkumar Mishra, Debapriya Das, Subrata Paul, A comprehensive review on power distribution network reconfiguration, *Energy Syst.* (2016) 1–58.
- [22] Dong Zhang, Zhengcai Fu, Liuchun Zhang, An improved TS algorithm for loss-minimum reconfiguration in large-scale distribution systems, *Electr. Power Syst. Res.* 77.5 (2007) 685–694.
- [23] M.M. Aman, G.B. Jasmon, A.H.A. Bakar, H. Mokhlis, Optimum network reconfiguration based on maximization of system loadability using

- continuation power flow theorem, *Int. J. Electr. Power Energy Syst.* 54 (2014) 123–133.
- [24] Mehdi. Rahmani-andebili, Simultaneous placement of DG and capacitor in distribution network, *Electr. Power Syst. Res.* 131 (2016) 1–10.
- [25] Qingfu Zhang, Li Hui, MOEA/D: A multiobjective evolutionary algorithm based on decomposition, *IEEE Trans. Evol. Comput.* 6 (2007) 712–731.
- [26] Qingfu Zhang, Wudong Liu, Li. Hui, The performance of a new version of MOEA/D on CEC09 unconstrained MOP test instances, *IEEE Congress Evol. Comput.* 1 (2009).
- [27] Shi-Zheng Zhao, Suganthan Ponnuthurai Nagaratnam, Zhang Qingfu, Decomposition-based multiobjective evolutionary algorithm with an ensemble of neighborhood sizes, *IEEE Trans. Evol. Comput.* 16.3 (2012) 442–446.
- [28] K. Miettinen, *Nonlinear Multiobjective Optimization*, vol. 12, Springer Science & Business Media, 2012, 2017.
- [29] Q. Jiang, L. Wang, X. Hei, G. Yu, Y. Lin, X. Lu, MOEA/D-ARA+ SBX: A new multi-objective evolutionary algorithm based on decomposition with artificial raindrop algorithm and simulated binary crossover, *Knowl.-Based Syst.* 107 (2016) 197–218.
- [30] Taher. Niknam, An efficient multi-objective HBMO algorithm for distribution feeder reconfiguration, *Expert Syst. Appl.* 38.3 (2011) 2878–2887.
- [31] Ching-Tzong Su, Chung-Fu Chang, Ji-Pyng Chiou, Distribution network reconfiguration for loss reduction by ant colony search algorithm, *Electr. Power Syst. Res.* 75.2 (2005) 190–199.
- [32] R.D. Zimmerman, C.E. Murillo-Sánchez, R.J. Thomas, *Matpower*, 2017 (Available at: <http://www.pserc.cornell.edu/matpower>).